

Fully-automated image processing software to analyze calcium traces in populations of single cells

Loo Chin Wong^a, Bo Lu^{a,1}, Kia Wee Tan^a, Marc Fivaz^{a,b,*}

^a DUKE-NUS Graduate Medical School, Program in Neuroscience and Neurobehavioral Disorders, 8 College Road, Singapore 169857, Singapore

^b Department of Physiology, School of Medicine, National University of Singapore (NUS), Singapore

ARTICLE INFO

Article history:

Received 21 July 2010

Received in revised form

16 September 2010

Accepted 19 September 2010

Available online 16 October 2010

Keywords:

Calcium

Imaging

STIM

SOCE

Segmentation

Software

ABSTRACT

Advances in fluorescence live cell imaging over the last decade have revolutionized cell biology by providing access to single-cell information in space and time. One current limitation of live-cell imaging is the lack of automated procedures to analyze single-cell data in large cell populations. Most commercially available image processing softwares do not have built-in image segmentation tools that can automatically and accurately extract single-cell data in a time series. Consequently, individual cells are usually identified manually, a process which is time consuming and inherently low-throughput.

We have developed a MATLAB-based image segmentation algorithm that reliably detects individual cells in dense populations and measures their fluorescence intensity over time. To demonstrate the value of this algorithm, we measured store-operated calcium entry (SOCE) in hundreds of individual cells. Rapid access to single-cell calcium signals in large populations allowed us to precisely determine the relationship between SOCE activity and STIM1 levels, a key component of SOCE. Our image processing tool can in principle be applied to a wide range of live-cell imaging modalities and cell-based drug screening platforms.

© 2010 Elsevier Ltd. All rights reserved.

1. Introduction

Live imaging offers the unique advantage of watching a biological system function over time. With the emergence of automated instrumentation and genetically encoded fluorescent biosensors, it is now theoretically possible to measure dynamic changes of multiple single-cell parameters, such as protein–protein interactions, signaling events, or transcriptional regulation, in large cell populations [1–5]. However, because of the complex nature of such single-cell readouts, data analysis is usually performed manually or semi-automatically for a few individual cells, raising the possibility of personal bias and inadequate statistical sampling.

Most commercially available image processing softwares lack built-in segmentation algorithms that can automatically detect individual cells and extract single-cell parameters in a time series. Some imaging softwares, such as MetaMorph for example, offer applications that segment cells based on a threshold intensity, but lack the ability to separate cells that are contacting one another, and thus perform poorly in dense cell populations. Consequently, most

users typically draw regions of interest (ROIs) manually to label individual cells, which dramatically lengthens data analysis and thus precludes analysis of large cell populations. Software packages that come with automated fluorescence microscopy platforms have more elaborated cell segmentation algorithms, but these are expensive and usually not integrated in applications that extract single-cell data in a time series.

Here, we present an image segmentation algorithm that reliably identifies individual cells in a field and measures fluorescent intensity over time. Our software uses the watershed transform to individuate cells touching each other, and thus performs well in dense cell populations. Our script is applicable to a wide range of live-cell imaging modalities, such as calcium imaging, bimolecular fluorescence complementation (BiFC), fluorescence energy transfer (FRET) or transcription reporter assays.

To demonstrate the use of our algorithm, we chose to measure Store-Operated Calcium Entry (SOCE) in hundreds of individual cells. SOCE is the major Ca^{2+} entry pathway in non-excitabile cells and is critical for a number of important cellular functions including motility, secretion and gene expression [6]. SOCE is regulated by Ca^{2+} depletion from the endoplasmic reticulum (ER), which is detected by the ER-localized Ca^{2+} sensor STIM1 [7,8]. STIM1 oligomerizes and migrates to ER-plasma junction sites upon store depletion, where it activates the Ca^{2+} channel ORAI1 at the plasma membrane, resulting in Ca^{2+} influx [7,9–14]. To demonstrate the value of automated single-cell analysis in large populations, we

* Corresponding author at: Duke-NUS Graduate Medical School Singapore, 8 College Road, Singapore 169857, Singapore. Tel.: +65 6516 7748.

E-mail address: marc.fivaz@duke-nus.edu.sg (M. Fivaz).

¹ Present address: Department of Physiology, Development and Neuroscience, University of Cambridge, Downing Street, Cambridge CB2 3DY, UK.

silenced STIM1 using a short hairpin RNA (shRNA) construct and correlated SOCE activity with STIM1 concentration in hundreds of individual cells.

2. Materials and methods

2.1. Reagents

The psiLv-H1TM shRNA expression vectors (co-expressing mCherry) were purchased from GeneCopoeiaTM. The sequence of the scrambled shRNA is CGATACTGAACGAATCGAT. The shRNA sequence against rat STIM1 is TCCAGGCAGGAAGAAGTTT. The STIM1 pAb was from Cell Signaling (#4916).

2.2. Cell culture and electroporation

Neuroscreen-1 cells (a clone derived from rat pheochromocytoma cells) were purchased from ATCC and grown in Dulbecco's Modified Eagle's Medium (high glucose) with 10% horse serum and 5% Fetal Bovine Serum (Invitrogen). To transfect Neuroscreen-1 cells with shRNA constructs, 1×10^5 cells were electroporated with 3 μ g of the respective DNA using the NeonTM Transfection System in 100 μ l of the NeonTM electroporation buffer (Invitrogen). The settings for the electroporation were as follow: 1410V Pulse Voltage, 30 ms Pulse Width, 1 Pulse Number. The cells were then seeded onto Lab-Tek Chambered Coverglass (Bio Lab/NUNC) and maintained for another 3 days in 5% CO₂ before imaging.

2.3. Live cell confocal imaging and image processing

See on-line supplementary methods.

3. Results and discussion

3.1. An image segmentation algorithm to identify individual cells in a field

We set out to develop a versatile image segmentation tool that reliably identifies cells in an image, based on a fluorescence signal. Our algorithm was designed to meet the following four criteria. (1) Touching cells should be accurately separated, allowing single-cell analysis of dense cell populations. (2) Cell segmentation should not require nuclear staining (a segmentation strategy that is widely used in commercial imaging processing algorithms), since this is not always compatible with live-cell imaging. (3) Segmentation should be easily implementable in time series, in order to extract time-dependent changes in single cell parameters. (4) The code should be user friendly and flexible (the user should have the possibility, if desired, to set segmentation parameters based on visual inspection). The script, termed ISA (for Image-based Segmentation Algorithm) was written in MATLAB using built-in functions of the image processing toolbox.

Fig. 1b shows a typical confocal fluorescence image of cells labeled with the calcium dye Fluo-4. There are ~150 cells in this field displaying a range of fluorescence intensities, many of which are in direct contact with neighboring cells. Separating touching objects in an image can be a challenging task in image processing. We applied the watershed transform to solve this problem. The watershed transform finds “catchment basins” and “watershed ridge lines” in an image by treating it as a surface where light pixels are high and dark pixels are low [15,16]. The workflow for marker-based watershed segmentation is depicted in Fig. 1a (see methods). The result of the watershed transform is shown in Fig. 1g. Each detected object is displayed using a pseudocolor scale

(Fig. 1g) or is numbered (Fig. 1h). Note that the software accurately separates cells that are in direct contact with each other (compare Fig. 1c with g and h). ISA detects 151 out of 153 cells present in this image, and separates touching cells with 89% accuracy.

3.2. Automated analysis of single-cell Ca²⁺ traces

We next used ISA to automatically detect single-cell Ca²⁺ changes in a time-lapse experiment. We chose to monitor store-operated Ca²⁺ entry (SOCE), an important Ca²⁺ entry pathway in non-excitable cells, which is regulated by Ca²⁺ depletion from intracellular stores [17]. SOCE is classically measured by a Ca²⁺ addback assay [7]. Cells loaded with the Ca²⁺ dye Fluo-4 are treated with thapsigargin to release Ca²⁺ from stores and activate SOCE (in the absence of extracellular Ca²⁺), which is then measured by addition of extracellular Ca²⁺. The Ca²⁺ addback assay exhibits a bimodal Ca²⁺ profile, the first peak corresponds to thapsigargin-evoked Ca²⁺ mobilization from stores, while the second peak represents Ca²⁺ entry through SOC channels (Fig. 2a–c). We modified our software to extract the average fluorescence intensity of each individual segmented cell, and compute changes of Ca²⁺ signals in a time series (see methods) (Fig. 2b). To determine how our software performs, we manually drew regions of interest (ROIs) in each of these cells and measured Ca²⁺ responses using metamorph (Fig. 2c). ISA-derived Ca²⁺ traces are quantitatively and qualitatively comparable to these obtained manually.

3.3. Single-cell correlation analysis of SOCE activity and STIM1 levels

We then used ISA to precisely determine the relationship between SOCE activity and levels of STIM1, an ER-localized calcium sensor that detects store depletion and activates SOCE [7,8]. To alter endogenous STIM1 concentration, we silenced STIM1 using a short hairpin RNA (shRNA) sequence co-expressed with the red fluorescent protein mCherry. When assayed by qRT-PCR, this shRNA reduces in average the STIM1 transcript in Neuroscreen-1 cells by ~65% (Supplementary Fig. 1a). Importantly, single-cell analysis of STIM1 knock down by immunocytochemistry shows that the extent of knock down strongly correlates with mCherry intensity (Supplementary Fig. 1b and c). Both Fluo-4 (green) and mCherry images (red) were acquired during the Ca²⁺ addback assay and cells were segmented based on mCherry fluorescence (Fig. 3a). Fluo-4 Ca²⁺ traces (for mCherry-expressing cells only) were then computed as described above. Since mCherry-expressing cells exhibit a wide-range of fluorescence intensities, analysis of a sufficiently large cell population should give access to single-cell SOCE responses for a broad spectrum of STIM1 concentrations. To increase the number of cells for this experiment, we acquired time-lapse data for up to four different fields in parallel using multi-position imaging (see methods). Fig. 3b shows single-cell and average Ca²⁺ profiles for a control shRNA sequence. The bimodal response is similar to that shown in Fig. 2. shRNA-mediated knock-down of STIM1 has no effect on thapsigargin-evoked Ca²⁺ release, but leads, in average, to a 60% reduction of the Ca²⁺ addback peak, indicating SOCE inhibition (Fig. 3c). Note, however, that single-cell responses upon Ca²⁺ addback are quite heterogeneous. Some cells show unaffected SOCE responses, while others exhibit no SOCE activity (Fig. 3c). To further explore the relationship between SOCE activity and STIM1 concentration, we plotted the maximum Fluo-4 intensity after Ca²⁺ addition (Ca²⁺ addback peak), as a function of mCherry intensity for each individual cell (Fig. 3e). We observed a strong negative correlation between SOCE activity and mCherry concentration. SOCE was unaffected, or mildly affected in cells weakly expressing mCherry

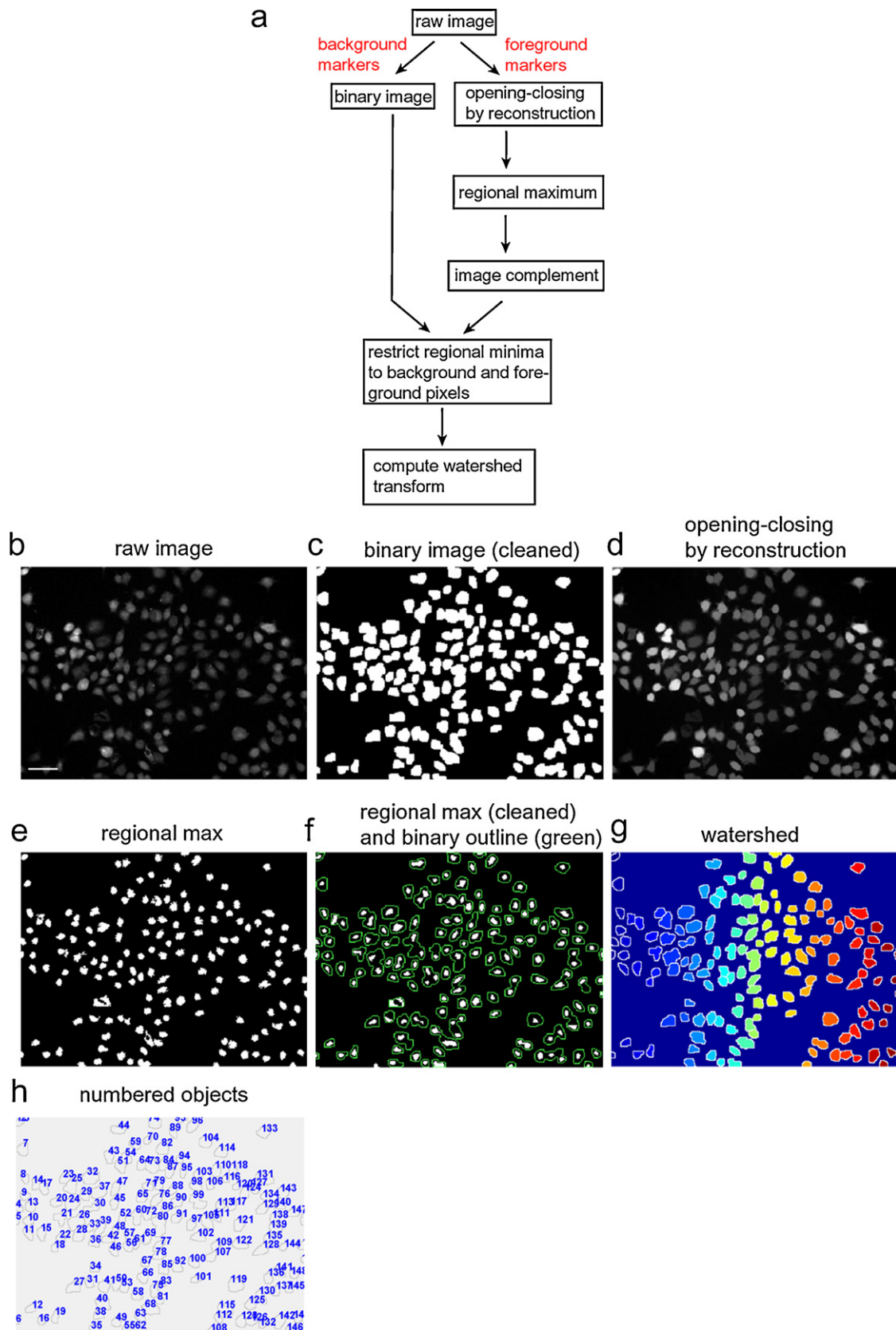


Fig. 1. Marker-based watershed segmentation of individual cells in a field. (a) Workflow for marker-based watershed segmentation (see text and methods). (b) Confocal image of Neuroscreen-1 cells loaded with Fluo4. (c) Cleaned binary image. (d) Processed image after opening-by-reconstruction and closing-by-reconstruction. (e) Identification of regional maxima. (f) Cleaned-up regional maxima are shown with the cell outline (green). (g) Result of watershed segmentation. Individual cells detected by the software are visualized according to a pseudocolor scale. (h) The same detected objects are numbered. Scale bar: 50 μm .

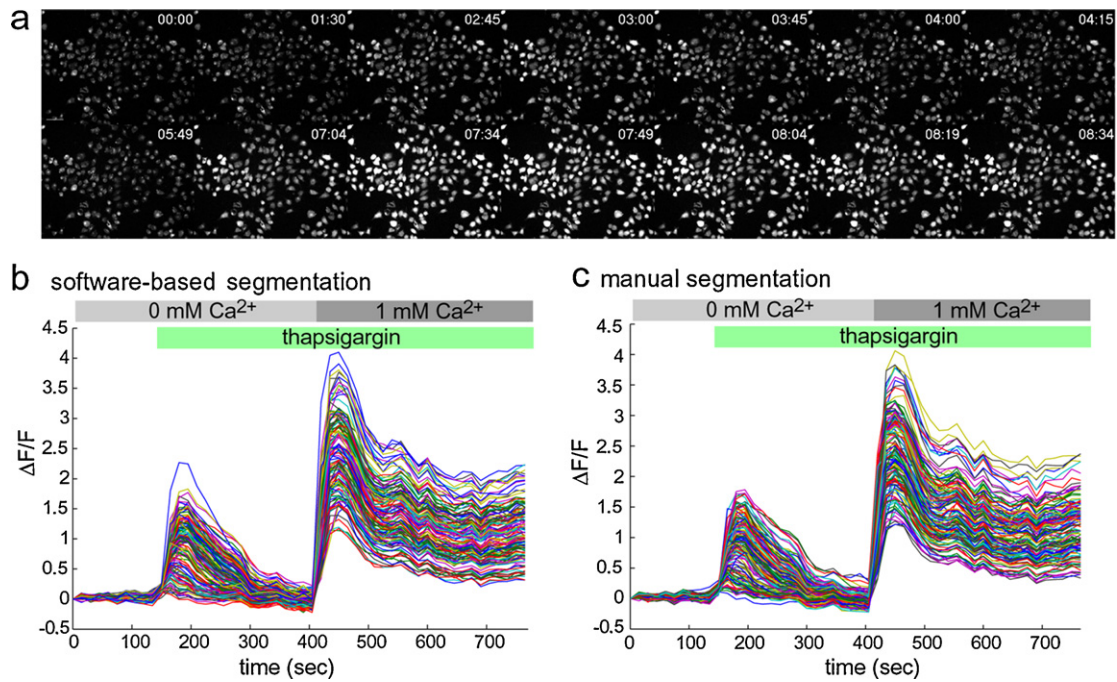


Fig. 2. Automated detection of single-cell Ca²⁺ signals in a time series. (a) Snapshots of a “Ca²⁺ addback” assay to monitor SOCE in Fluo4-loaded Neuroscreen-1 cells. Note the biphasic calcium increase triggered by thapsigargin-evoked Ca²⁺ release and Ca²⁺ influx through SOC channels. Time is in minutes and seconds (scale bar: 50 μ m). (b) Automated display of single-cell Ca²⁺ traces derived from cells detected by the watershed algorithm. (c) Manual detection of single-cell Ca²⁺ responses.

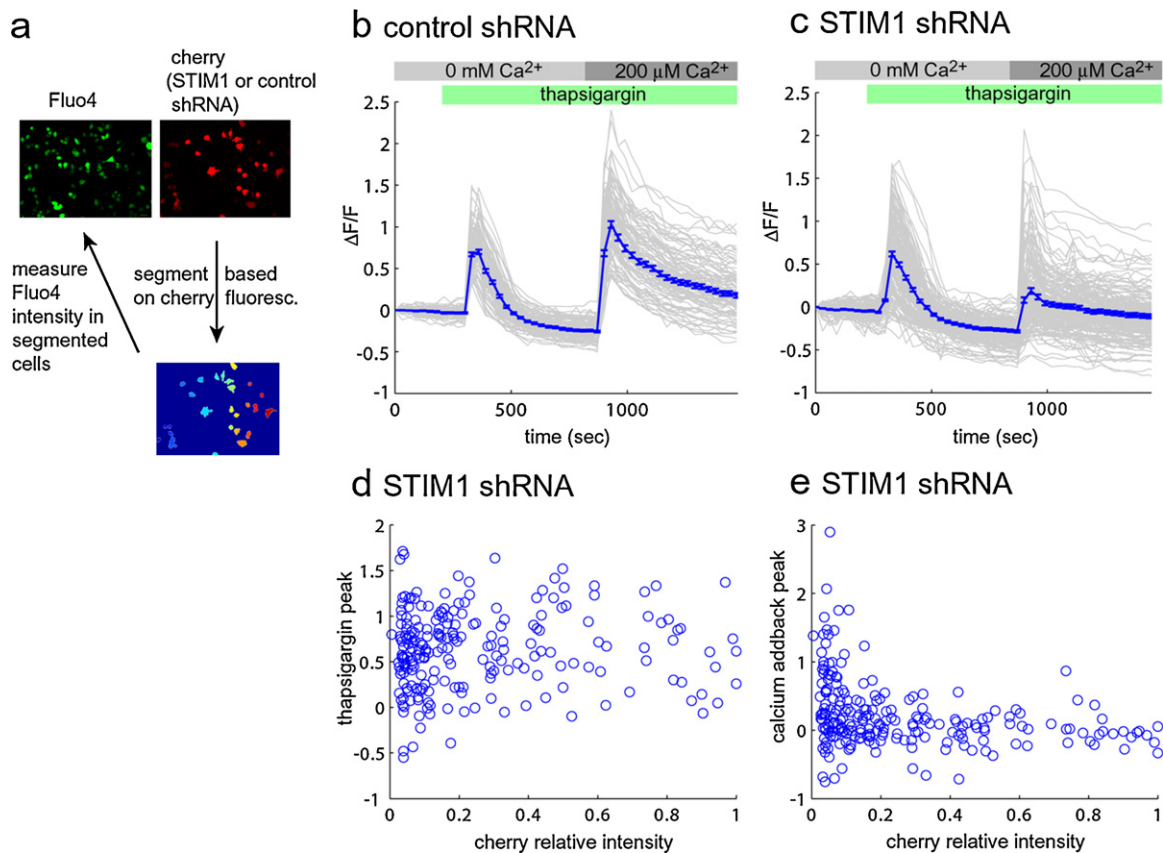


Fig. 3. Single-cell correlation of SOCE activity with STIM1 expression levels. Ca²⁺ addback assay in cells expressing a scrambled (b) or STIM1 (c–e) shRNA construct. (a) Segmentation is performed on mCherry-expressing cells (indicator of shRNA expression). Fluo4 measurements are then carried out in cells identified based on mCherry expression. Individual (light grey) and average (blue) Ca²⁺ profiles in cells expressing the control shRNA (b) or the STIM1 shRNA (c). The error bar represents the standard error of the mean. $n > 150$ cells for each data set. (d) Thapsigargin-evoked Ca²⁺ release plotted as a function of mCherry intensity (reflecting STIM1 shRNA expression). (e) SOCE activity (measured by the peak Fluo4 intensity after Ca²⁺ addback) expressed as a function of mCherry intensity (reflecting STIM1 shRNA expression). Each blue circle represents a single cell.

(below ~20% of maximal mCherry intensity), but was almost completely abrogated above a certain mCherry intensity (above ~30% of maximal mCherry intensity). As a control, we plotted the peak Fluo-4 fluorescence in response to thapsigargin addition (thapsigargin peak) as a function of mCherry concentration and observed no correlation (Fig. 3d), indicating that STIM1 knock-down does not alter thapsigargin-evoked Ca^{2+} release. Similarly, no correlation was observed between the amplitude of thapsigargin-evoked Ca^{2+} release or SOCE and mCherry intensity in cells transfected with a control shRNA (Supplementary Fig. 2a, b). These data illustrate the value of ISA to rapidly and accurately quantitate a knock-down phenotype in hundreds of individual cells.

In conclusion, we have developed an image segmentation algorithm (ISA) that reliably detects single cells in dense populations. Our software was optimized to segment cells based on cytoplasmic fluorescence patterns and can thus be applied to a wide-range of available fluorescent biosensors. Here, we have applied ISA to calcium imaging data and have shown that our software identifies individual cells and extracts single-cell Ca^{2+} signals in time series with minimal error. ISA can segment cells based on multiple fluorescent readouts, thereby allowing the identification of distinct cell populations in dual- or multiple-color imaging experiments (Fig. 3). Our algorithm can easily be used in a “batch processing” mode, providing automated analysis of multiple time series derived, for example, from multi-position imaging.

Conflict of interest

None.

Acknowledgments

The authors thank Tony VanDongen, Mathijs Voorhoeve and Lynette Lim for critical reading of the manuscript. We are grateful to all Fivaz Lab members for their valuable input and feedback. This work was supported by the Singapore Ministry of Education Academic Research Fund (MOE Tier 2, T208B3101) and by the Duke-NUS Signature Research Program funded by the Agency for Science, Technology and Research, Singapore, and the Ministry of Health, Singapore.

Appendix A. Supplementary data

Supplementary data associated with this article can be found, in the online version, at doi:10.1016/j.ceca.2010.09.008.

References

- [1] B. Neumann, T. Walter, J.K. Heriche, J. Bulkescher, H. Erfle, C. Conrad, P. Rogers, I. Poser, M. Held, U. Liebel, C. Cetin, F. Sieckmann, G. Pau, R. Kabbe, A. Wunsche, V. Satagopam, M.H. Schmitz, C. Chapuis, D.W. Gerlich, R. Schneider, R. Eils, W. Huber, J.M. Peters, A.A. Hyman, R. Durbin, R. Pepperkok, J. Ellenberg, Phenotypic profiling of the human genome by time-lapse microscopy reveals cell division genes, *Nature* 464 (2010) 721–727.
- [2] S.G. Megason, S.E. Fraser, Imaging in systems biology, *Cell* 130 (2007) 784–795.
- [3] P. Vitorino, T. Meyer, Modular control of endothelial sheet migration, *Genes Dev.* 22 (2008) 3268–3281.
- [4] M. Bickle, The beautiful cell: high-content screening in drug discovery, *Anal. Bioanal. Chem.* 398 (2010) 219–226.
- [5] F. Zanella, J.B. Lorens, W. Link, High content screening: seeing is believing, *Trends Biotechnol.* 28 (2010) 237–245.
- [6] A.B. Parekh, J.W. Putney Jr., Store-operated calcium channels, *Physiol. Rev.* 85 (2005) 757–810.
- [7] J. Liou, M.L. Kim, W.D. Heo, J.T. Jones, J.W. Myers, J.E. Ferrell Jr., T. Meyer, STIM is a Ca^{2+} sensor essential for Ca^{2+} -store-depletion-triggered Ca^{2+} influx, *Curr. Biol.* 15 (2005) 1235–1241.
- [8] J. Roos, P.J. DiGregorio, A.V. Yeromin, K. Ohlsen, M. Lioudyno, S. Zhang, O. Safrina, J.A. Kozak, S.L. Wagner, M.D. Cahalan, G. Velicelebi, K.A. Stauderman, STIM1, an essential and conserved component of store-operated Ca^{2+} channel function, *J. Cell Biol.* 169 (2005) 435–445.
- [9] J. Liou, M. Fivaz, T. Inoue, T. Meyer, Live-cell imaging reveals sequential oligomerization and local plasma membrane targeting of stromal interaction molecule 1 after Ca^{2+} store depletion, *Proc. Natl. Acad. Sci. U.S.A.* 104 (2007) 9301–9306.
- [10] R.M. Luik, B. Wang, M. Prakriya, M.M. Wu, R.S. Lewis, Oligomerization of STIM1 couples ER calcium depletion to CRAC channel activation, *Nature* 454 (2008) 538–542.
- [11] R.M. Luik, M.M. Wu, J. Buchanan, R.S. Lewis, The elementary unit of store-operated Ca^{2+} entry: local activation of CRAC channels by STIM1 at ER-plasma membrane junctions, *J. Cell Biol.* 174 (2006) 815–825.
- [12] S. Feske, Y. Gwack, M. Prakriya, S. Srikanth, S.H. Puppel, B. Tanasa, P.G. Hogan, R.S. Lewis, M. Daly, A. Rao, A mutation in Orai1 causes immune deficiency by abrogating CRAC channel function, *Nature* 441 (2006) 179–185.
- [13] M. Vig, C. Peinelt, A. Beck, D.L. Koomoa, D. Rabah, M. Koblan-Huberson, S. Kraft, H. Turner, A. Fleig, R. Penner, J.P. Kinet, CRACM1 is a plasma membrane protein essential for store-operated Ca^{2+} entry, *Science* 312 (2006) 1220–1223.
- [14] S.L. Zhang, A.V. Yeromin, X.H. Zhang, Y. Yu, O. Safrina, A. Penna, J. Roos, K.A. Stauderman, M.D. Cahalan, Genome-wide RNAi screen of Ca^{2+} influx identifies genes that regulate Ca^{2+} release-activated Ca^{2+} channel activity, *Proc. Natl. Acad. Sci. U.S.A.* 103 (2006) 9357–9362.
- [15] <http://blogs.mathworks.com/steve/2006/06/02/cell-segmentation/>.
- [16] <http://www.mathworks.nl/products/image/demos.html?file=/products/demos/shipping/images/ipexwatershed.html>.
- [17] J.W. Putney Jr., A model for receptor-regulated calcium entry, *Cell Calcium* 7 (1986) 1–12.